

# Can Quasi-Particles Tunnel Through A Barrier?

Elad Shopen<sup>1</sup>, Yuval Gefen<sup>2</sup>, and Yigal Meir<sup>1,3</sup>

<sup>1</sup> *Physics Department, Ben-Gurion University, Beer Sheva 84105, Israel*

<sup>2</sup> *Department of Condensed Matter Theory, The Weizmann Institute of Science, Rehovot 76100, Israel*

<sup>3</sup> *The Ilse Katz Center for Meso- and Nano-scale Science and Technology, Ben-Gurion University, Beer Sheva 84105, Israel*

This is a qualitative description of a systematic analysis carried out by us<sup>1</sup>. We address the question of whether fractionally charged particles, in the context of the fractional quantum Hall effect (FQHE) can tunnel through a potential barrier (around which the density of the quantum Hall liquid is practically zero). Setting the barrier in a multiply-connected FQHE geometry removes the "global constraint" which prohibits such tunnelling. We have performed a microscopic analysis of adiabatic charge pumping and tunnelling in a torus geometry. Below we summarize our analysis in semi-qualitative terms. We also propose a setup—different from the torus geometry—amenable to experimental verification.

## 1 Motivation

A common approach for observing elementary charge carriers within fractional quantum Hall effect (FQHE) systems is through tunnelling. It has been pointed out<sup>2,3</sup> that QP tunnelling is distinctly different from electron tunnelling. Perturbative renormalization-group analysis<sup>4</sup> has indicated that in the weak backscattering limit interedge tunnelling through the FQHE liquid is dominated by QP tunnelling. These predictions have been confirmed by experiments<sup>5</sup>. In the opposite limit of strong backscattering (nearly disconnected FQHE systems coupled by weak tunnelling through an insulator), the same RG analysis would have predicted that tunnelling should be dominated again by QP tunnelling. Common wisdom, however, has it that in that limit only electron tunnelling is possible. The rationale for that goes as follows: consider two FQHE puddles weakly connected through tunnelling. The total number of electrons on each puddle ( $N_R, N_L$  respectively) is a (nearly) good quantum number; hence it must be an integer. QP tunnelling would render this number non-integer, therefore such a process must be excluded<sup>6</sup>.

Our starting point here is to note that there are setups where the above mentioned "global constraint" (i.e. the number of electrons on each side of the barrier being an integer) does not exclude a-priori QP tunnelling through a potential barrier. The common wisdom alluded to above needs then to be re-examined. Studying these setups is particularly interesting in view of recent experimental results<sup>7</sup> which suggest the coexistence of both electron and QP tunnelling under rather strong backscattering conditions. Throughout this paper we will refer to the  $\nu = 1/m$  FQHE.

## 2 Annular Geometry

The simplest geometry, probably most amenable to experimental verification, is that of the annulus shown in Fig. 1.a.

One of the arms of the annulus includes a tunnel barrier void of Hall liquid. Tunnelling may then occur through this barrier. We now present a few qualitative insights concerning this setup. The obvious approach to study this system is by employing the chiral Luttinger liquid model to describe the low energy dynamics at the edges. Fig. 1.b shows chiral edges which are topologically equivalent to the original system. Scattering due to the tunnelling barrier (dashed line) is always forward. The zero frequency transmission probability is therefore  $T = 1$  implying that the (zero frequency) quantum shot-noise spectrum  $S_2 = V(e^2/h)T(1 - T)$  vanishes. Finite

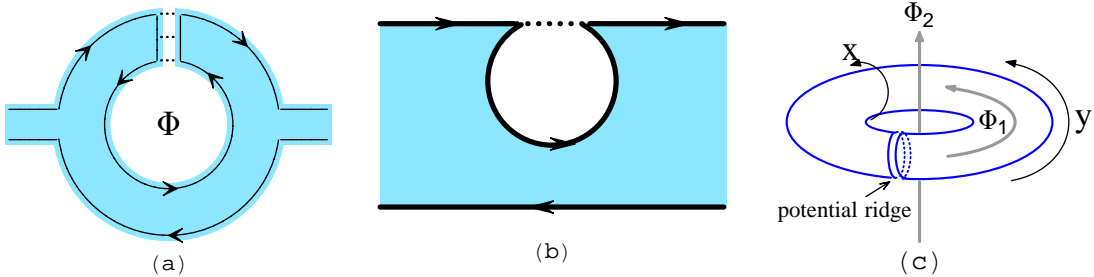


Figure 1: Setups for studying possible QP tunnelling through an insulator. (a) An annular geometry. Solid lines indicate the directions of the edge currents; dotted lines—tunnelling trajectories. The shaded area represents the  $\nu = 1/m$  FQHE liquid. (b) An equivalent geometry in terms of edge and tunnelling currents. (c) A torus geometry.  $\Phi_1, \Phi_2$  are the two gauge fluxes.

frequency noise may, nevertheless, be generated. The mechanism to this is that the "loop" at the barrier may be considered as a capacitor which gets stochastically charged and discharged. In other words, fluctuations in the form of charged wave-packets coming from left may follow several windings around this loop before leaking to the right-hand-side of the edge. While the d.c. conductance will *not* be sensitive to an Aharonov-Bohm (AB) flux threading the loop (the zero frequency transmission is anyway 1), the finite frequency noise *will* be sensitive to that flux. We expect the flux periodicity of the noise to depend on whether the tunnelling is dominated by quasi-particles or electrons.

### 3 Charge and Aharonov-Bohm Periodicity

The subtle relation between the charge of the elementary carriers (or the elementary charge participating in tunnelling) and the AB periodicity in multi-connected structures has been elucidated by Thouless and Gefen<sup>3</sup> for the case of an annular geometry. In general the electronic ground state (in the FQHE regime) may be multiply degenerate, forming a structure of intersecting flux periodic minibands. Tunnelling gives rise to avoided crossing, cf. Fig 2.a where the  $m = 3$  case is depicted. This figure is quite generic, as shown by our present analysis. Quasi-particle-tunnelling-generated minigaps give rise to  $\Phi_0 \equiv hc/e$  periodicity. If only electron tunnelling is permitted the corresponding gap gives rise to  $3\Phi_0$  periodicity. Note that with  $e^* = e/3$  this is equivalent to  $hc/e^*$  periodicity. Thus, the flux periodicity is a clear-cut mean to identify the charge associated with tunnelling.

### 4 Formulating the Challenge and Working Out the Problem – an Outline of the Analysis

The question at the heart of the dilemma here is whether fractionally charged quasi-particles can indeed tunnel through a potential barrier. Should the answer to this be in the affirmative, the next step is to study the *magnitude* of the quasi-particle tunnelling amplitude,  $\mathcal{T}_{qp}$ , as function of the relevant parameters, and compare it with the amplitude for electron tunnelling,  $\mathcal{T}_e$ . In view of Fig 2.a, these amplitudes are proportional to the respective QP and electron gaps indicated there. As was emphasized above the suppression of  $\mathcal{T}_{qp}$  will lead to the change of the flux periodicity from  $\Phi_0$  to  $m\Phi_0$ . A particularly intriguing question here is the role of impurities. It turns out that in general their presence enhances the above tunnelling amplitudes. But this will be discussed elsewhere.

We now present a qualitative description of the main steps of the analysis carried out by us:

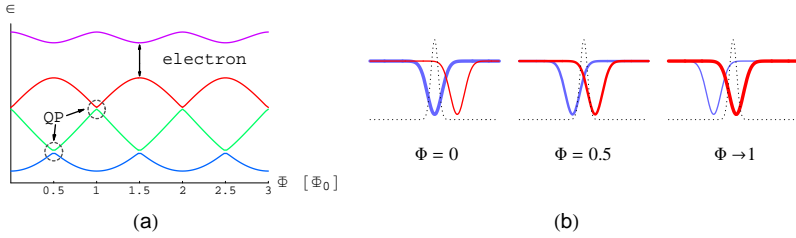


Figure 2: Relation between charge and Aharonov-Bohm periodicities. (a) Energies of selected many-body configurations as function of AB flux. Finite matrix elements for QP tunnelling give rise to gaps in the adiabatic spectrum ("avoided crossings"), rendering the adiabatic variation of the ground-state energy vs. flux  $\Phi_0$ -periodic. In the absence of such matrix elements electron tunnelling gives rise to a  $m\Phi_0$ -periodicity. (b) Density profiles (solid lines) of two many-body configurations on the torus. These configurations slide continuously as the flux  $\Phi_1$  is modified adiabatically. The minimum energy configuration shifts from the first to the second configuration, depending on whose density minimum coincides with the potential ridge (dotted line).

- (i) We recall the structure and analytic properties of the lowest-Landau-level single electron wave-functions defined on the surface of a torus (whose periodic coordinates are  $x, y$ ) in the presence of a strong perpendicular magnetic field ( $N_\Phi$  flux quanta). Likewise we review the many-body wave-functions in the FQHE regime<sup>8,9</sup>. We note that these wave-functions depend on the gauge fluxes,  $\Phi_1$  and  $\Phi_2$ , threading the torus (cf. Fig.1.c).
- (ii) We generalize the many-body wave-functions to include  $N_h$  localized quasi-holes at points  $z_{01}, z_{02}, \dots, z_{0N_h}$ . These coordinates can be thought of as the locations of point-like impurities. Alternatively these are the quasi-holes generated by inserting extra  $N_h$  flux quanta through the surface, on top of the  $N_\Phi$  fluxons<sup>10</sup> (the number of electrons  $N = (N_\Phi - N_h)/m$ ).
- (iii) Many-body wave-functions with  $N_h$  localized holes are now expressed in terms of  $N_h$  "extended holes". The latter refers to wave-functions in which certain single electron states (certain quasi momentum components) are excluded. Consecutive extended holes form a "dry swath" (a minimum or even a zero-density regime) of circular symmetry. There are a number of degenerate many-body states characterized by the location of the dry swath.
- (iv) We now introduce, on top of the torus surface, a potential ridge, Fig. 1.c. This ridge removes the degeneracy of the many-body states. The wave-function with the dry swath coinciding with the ridge has the lowest energy (Fig 2.b,  $\Phi = 0$ ).
- (v) By adiabatically varying the gauge flux  $\Phi_1$  we cause the incompressible liquid (and the dry swath) represented by the many-body wave-function  $\Psi_n$  to rigidly slide around the torus in the  $y$ -direction. Note that this sliding implies that the liquid (the incompressible "sea") may climb up and down the ridge. This is still not what we would call tunnelling. The trace of the energy vs.  $\Phi_1$  ( $E_n(\Phi_1)$ ) is modulated with the flux. Also – as the swath of  $\Psi_n$  moves away from the ridge, the swath of another state,  $\Psi_{n+1}$ , replaces it, resulting in  $E_n(\Phi_1)$  and  $E_{n+1}(\Phi_1)$  intersecting. The degeneracy of these two states at the intersection point is not removed:  $\Psi_n$  and  $\Psi_{n+1}$  differ in their total quasi momentum (TQM), and the circularly symmetric ridge cannot provide a matrix element to remove the degeneracy between them.
- (vi) We now break the local circular symmetry of the problem by introducing an extra potential (e.g., an additional  $\delta$ -function potential on top of the ridge). This may now generate matrix elements among the sliding states whose energy traces intersect. These matrix elements, leading to gaps in the spectrum (cf. Fig 2.a) are manifestations of tunnelling.
- (vii) Physically the tunnelling can be understood in the following terms. By adiabatically varying  $\Phi_1$  the rigid electron configuration associated with  $\Psi_n$  is pushed (pumped) around the torus. Increasing  $\Phi_1$  by  $\Phi_0$  will push the state by one guiding center, *i.e.* will effectively push a QP

of charge  $1/m$  across the swath. This will result in another many-body state,  $\Psi_{n+1}$ . If the circular-symmetry breaking potential alluded to above generates a (significant) finite matrix element between these two states, we identify the process as an effective QP tunnelling across the ridge (corresponding to the QP gap in Fig 2.a). Otherwise we need to increase  $\Phi_1$  by  $m\Phi_0$ , pushing the charge of an electron across the ridge, to generate a (significant) matrix element between  $\Psi_n$  and  $\Psi_{n+m}$  (an electron gap, cf. Fig 2.a).

(viii) Once the magnitudes of the electron and the QP tunnelling matrix elements are evaluated, we can find the crossover (as function of the torus geometrical characteristics and the thickness of the ridge potential barrier) between the two processes.

## 5 Results

Below we present some of our results. First we observe (in our multiply-connected geometry, no "global constraint") a non-vanishing amplitude for QP tunnelling. The interesting question then is whether the effect is mesoscopic or is it also observable in the thermodynamic limit. This can be answered by studying how the tunnelling amplitudes for electrons and QPs depend on system's size. The result is quite striking: we have found that tunnelling of electrons is practically unaffected by increasing the size of the system (keeping the potential barrier unchanged), while the tunnelling amplitude for QPs vanishes (Gaussian-like). Hence tunnelling of QPs *is* a mesoscopic effect. Such tunnelling involves the entire electron sea and is a manifestation of the overlap between the initial and final states of this sea. Let us show this more quantitatively: the tunnelling amplitude is given by  $\mathcal{T}_k \equiv \langle \Psi_n | V | \Psi_{n+k} \rangle$ , where  $\Psi_n$  is a Laughlin correlated wave function with extended holes (the dry swath whose center is the  $n$ -th single particle state);  $V$  is the symmetry breaking potential, taken for convenience to be a Dirac delta-function  $\delta(x)$  (this specific choice does not modify our qualitative results);  $k = 1, m$  correspond to QP and electron tunnelling respectively. The size of the system may be increased by increasing the number of particles and flux quanta, keeping the occupation at the sea  $1/m$ . We first present results for a narrow circular ridge ( $N_h = 1$ ). Fig 3.a-b depict our results for  $N = 2, \dots, 6$ . We find for  $m = 3$

$$(\text{QP}) \quad \mathcal{T}_1 \sim e^{-\alpha L_2^2/\ell_H^2} \quad (1)$$

$$(\text{electron}) \quad \mathcal{T}_3 \sim \text{constant (as function of } L_2 \text{)} , \quad (2)$$

with  $\alpha \approx 1/14$ . Here  $L_2$  is the torus length and  $\ell_H = \sqrt{\hbar c/eB}$  the magnetic length.

It is clear that tunnelling of electrons is system size independent (i.e., it does not depend on the length – in the  $y$ -direction – of the sea), as opposed to QP tunnelling. While QP tunnelling through the barrier does exist, it is suppressed with the linear size of the electron sea *as if* the QP tunnelling takes place through the sea.

How can one understand this result qualitatively? Let us begin with QPs. The extension to electrons is then straightforward. The tunnelling amplitude  $\mathcal{T}_1$  involves  $\Psi_n$  and  $\Psi_{n+1}$ . The difference in TQM between these two states is  $N$  (the latter being the number of electrons):  $\Psi_{n+1}$  is obtained from  $\Psi_n$  by increasing the quasi momentum of each single particle component of the many-body wave-function by one, rendering the overall change of the TQM equal to the number of electron,  $N$ . Since the potential  $V$  is a single particle operator,  $\langle \Psi_n | V | \Psi_{n+1} \rangle$  is proportional to the product of single particle states whose quasi momentum difference is  $N$ . Let us approximate a single particle state by a Gaussian  $\sim e^{-(y-y_c)^2/2\ell_H^2}$ , with the guiding center at  $y_c$ . Adjacent guiding centers are distanced  $L_2/N_\Phi$  from one another. The guiding centers alluded to above are a distance  $N(L_2/N_\Phi) \approx L_2/m$  apart ( $m = 3$  is the inverse of the filling factor,  $N_\Phi = mN + 1$ ). Subsequently  $\langle \Psi_n | V | \Psi_{n+1} \rangle \sim \int e^{-y^2/2\ell_H^2} e^{-(y-L_2/m)^2/2\ell_H^2} dy \sim e^{-(L_2/2m)^2}$ .  $\mathcal{T}_1$  was previously calculated by Auerbach<sup>11</sup> for a cylindrical geometry vis-a-vis tunnelling of QPs through a quantum Hall liquid. The present discussion applies for Auerbach setup as well.

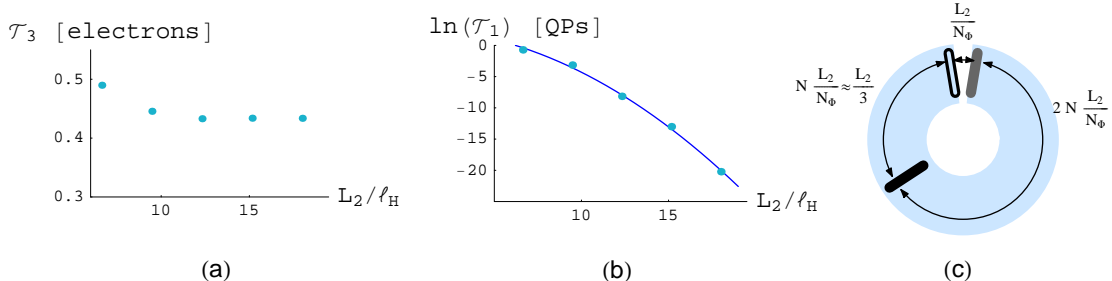


Figure 3: Dependence of tunnelling amplitudes on system's size. Data shown refer to a single extended hole,  $N = 2, \dots, 6$ . (a) For electrons  $\mathcal{T}_3$  is practically constant while (b) for QPs  $\mathcal{T}_1$  strongly decreases  $\sim e^{-\alpha L_2^2}$  with the linear size of the torus (all lengths are measured in units of  $\ell_H$ , the magnetic length). (c) Insight on the difference between electron and QP tunnelling: the empty box (just to the left of the potential ridge) denotes the location of the extended hole of the initial state. The tunnelling of a QP (an electron) involves initial and final many-body states, whose TQMs differ by  $N$  ( $3N$ ). The black (grey) box denotes the location of the extended hole following QP (electron) tunnelling. The respective matrix elements involve the overlap of two single particle states (Gaussians) whose distance is  $N L_2/N_\Phi \sim L_2/3$  (for electrons  $3N L_2/N_\Phi \bmod(L_2) = L_2 N_h/N_\Phi \ll L_2$ ). Thus for QPs the tunnelling matrix element scales as  $e^{-(L_2/3)^2/4}$ , while for electrons  $\sim e^{-(L_2/N_\Phi)^2/4}$  independent of  $L_2$  (note that  $L_2 \propto N_\Phi$ ).

This estimate verifies the Gaussian-like decrease, however the actual decay is stronger:  $m$  rather than  $m^2$  in the exponential. This is due to the normalization and combinatorial factors of the many-body wave-functions involved. It can be *pictorially* described as a QP performing  $m$  hops each a distance  $L_2/m$ . As each hop involves a decaying factor of  $e^{-(L_2/m)^2}$ , one reproduces the  $e^{-(L_2/2)^2/m}$  factor of Auerbach. We speculate that the  $1/14$  factor alluded to above approaches  $\alpha = 1/12$  at larger values of  $L_2$ .

Electrons tunnelling involves many-body states  $\Psi_n$  and  $\Psi_{n+m}$ , with TQM difference of  $mN$ . The guiding centers of the single particle wave-functions whose overlap we address are a distance  $(mN)(L_2/N_\Phi)$  apart. But as we are studying a torus, distances are defined modulo  $L_2$ , hence  $(mN)(L_2/N_\Phi) \bmod(L_2) = L_2/N_\Phi$ , which is system size independent (recall that  $N_\Phi = mN + 1 = L_1 L_2/\ell_H^2$ ). The physics discussed here is depicted (for  $m = 3$ ) in Fig 3.c.

Extending our study to thicker ridges (i.e., increasing the number of extended holes) supports the above conclusions- tunnelling of QPs practically does not depend on  $L_{\text{barrier}}$ , the barrier thickness, while electron tunnelling decreases as  $e^{-(L_{\text{barrier}}/2)^2}$ . A more careful analysis should account for the fact that electrons can tunnel through both- the barrier and the quantum Hall liquid, the latter depends Gaussian-like on the liquid length  $L_{\text{liquid}}$ ,  $\sim e^{-(L_{\text{liquid}}/2)^2}$ . This latter correction to electron tunnelling is sub-dominant to QPs tunnelling<sup>11</sup>.

A rough estimate for the crossover between electron and QP dominated tunnelling regimes, writing  $\mathcal{T}_1 = e^{-(L_{\text{liquid}}/2)^2/m}$  and  $\mathcal{T}_3 = e^{-(L_{\text{liquid}}/2)^2} + e^{-(L_{\text{barrier}}/2)^2}$  (this ignores pre-exponential prefactors). Fig 4 depicts the crossover curve, in fair agreement with a numerical calculation of  $\ln(\mathcal{T}_3/\mathcal{T}_1)$ . We believe that the experimental study of such an electron-to-QP crossover in multiply connected systems (e.g., an annulus) is now feasible.

Upon completion of this work we have learned of the manuscript by M. Helias and D. Pfannkuche, cond-mat/0403126. In this work numerical evidence for the occurrence of quasi-particle tunnelling near a potential saddle-point is reported.

## 6 Acknowledgment

We acknowledge useful discussions with F.D.M. Haldane, B.I. Halperin, M. Heiblum, A.D. Mirlin and D.J. Thouless. This work was supported in part by the US-Israel binational science

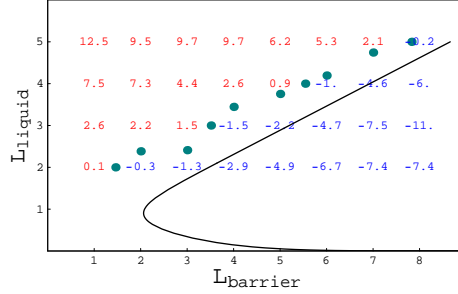


Figure 4:  $\chi \equiv \ln(\mathcal{T}_3/\mathcal{T}_1)$  (ratio of electron to QP tunnelling amplitudes) for the torus. Numerically computed values of  $\chi$  are indicated. The lengths of the barrier and the "sea" are measured in units of  $L_2/N_\Phi$ . Thick dots mark the (numerically interpolated) positions of  $\chi = 0$ . The solid curve marks the crossover between electron-to-QP-dominated tunnelling and is in agreement with our numerical data. This crossover curve is based on a simplified picture whereby the electron tunnel amplitude is the sum of tunnelling processes through the barrier and the sea which scale respectively as  $\sim e^{-L_{barrier}^2/4}$  and  $\sim e^{-L_{liquid}^2/4}$ ; QP tunnelling scale as  $\sim e^{-L_{liquid}^2/4m}$  ( $m = 1/\nu$ ).

foundation (BSF), by the Israel Science Foundation (ISF) of the Israel Academy of Science, and by the Alexander von Humboldt Foundation (through the Max Planck Award). Y.M. was supported at the WIS by the Albert Einstein Minerva Center (BMBF).

## References

1. E. Shopen *et. al.*, to be published.
2. S. A. Kivelson and V. L. Pokrovsky, *Phys. Lett. B* **40**, 1373 (1989); S. Kivelson, *Phys. Rev. Lett.* **65**, 3369 (1990); J. A. Simmons, H. P. Wei, L. W. Engel, D. C. Tsui and M. Shayegan, *Phys. Rev. Lett.* **63**, 1731 (1989); J. A. Simmons, S. W. Hwang, D. C. Tsui, H. P. Wei, L. W. Engel, and M. Shayegan, *Phys. Lett. B* **44**, 12933 (1991); V. J. Goldman and B. Su, *Science* **267**, 1010 (1995).
3. D.J. Thouless and Y. Gefen, *Phys. Rev. Lett.* **66**, 806 (1991); Y. Gefen and D. J. Thouless, *Phys. Lett. B* **47**, 10423 (1993).
4. K. Moon, H. Yi, C.L. Kane, M. Girvin and M.P.A. Fisher, *Phys. Rev. Lett.* **71**, 4381 (1993); M.P.A. Fisher and L.I. Glazman, *cond-mat/9610037*.
5. R. de-Picciotto, M. Reznikov, M. Heiblum, V. Umansky, G. Bunin and D. Mahalu, *Nature* **389**, 162 (1997); L. Saminadayar, D.C. Glattli, Y. Jin and B. Etienne, *Phys. Rev. Lett.* **79**, 2526 (1997).
6. To be more precise, one may tune the relative chemical potentials of the two puddles such that the last occupied discrete level on, say, the right-hand-side, is aligned with the first vacant level on the left; indeed,  $N_L, N_R$  need not be integers then. Nevertheless there is no indication that as function of the relative gate voltage they show a stepwise structure at  $1/m, 2/m, \dots$ , which would be a clear indication of QP tunnelling.
7. E. Comرت, Y.C. Chung, M. Heiblum, V. Umansky and D. Mahalu, *Nature* **416**, 5151 (2002); Y.C. Chung, M. Heiblum and V. Umansky, *condmat/0305325*.
8. D. Yoshioka, B.I. Halperin and P.A. Lee, *Phys. Rev. Lett.* **50**, 1219 (1983).
9. F.D.M. Haldane and E.H. Rezayi, *Phys. Lett. B* **31**, 2529 (1985).
10. Many-body states on a torus with a single localized hole have been introduced in Ref. <sup>9</sup>.
11. A. Auerbach, *Phys. Rev. Lett.* **80**, 817 (1998).